Journal of Molecular Liquids 411 (2024) 125702

Contents lists available at ScienceDirect

Journal of Molecular Liquids

journal homepage: www.elsevier.com/locate/molliq

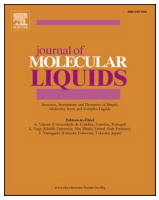

Radiation and nanoparticle interaction for enhanced light absorption and heat conversion

Oguzhan Kazaz [a], Nader Karimi [a,b], Manosh C. Paul [a,*]

[a] Systems, Power & Energy Research Division, James Watt School of Engineering, University of Glasgow, Glasgow G12 8QQ, UK
[b] School of Engineering and Materials Science, Queen Mary University of London, London E1 4NS, UK

ARTICLE INFO

Keywords:
Radiation-nanoparticle interaction
Nanofluids
Direct absorption
Heat transfer enhancement
Photothermal conversion and storage
Brownian motion

ABSTRACT

The photo-thermal conversion performance (PTCP) of water-based nanofluids in a volumetrically heated solar collector (VHSC) is evaluated. The influences of nanoparticle volume concentration (NVC), particle size, Reynolds number, operating temperature, and collector geometry on the PTCP are numerically investigated. The utilization of nanoparticles and improving their concentration is found to enhance the photo-thermal conversion efficiency (PTCE) of the collector by augmenting the energy from the sun of the working fluid due to the radiation-nanoparticle interactions. The PTCE enhancement of Graphite, TiO_2 and Ag nanoparticles dispersed in water is respectively 1.37, 1.33 and 1.29 times better, compared to that of water. This is further augmented by adding MgO nanoparticles to TiO_2, Graphite and Ag particles, resulting in 1.69, 1.67 and 1.59x improved efficiency. Enhancing the flow rate of the fluids also contributes to the PTCE by reducing the losses of thermal from the collector to the ambient. Besides, the enhanced nanoparticle size increases the overall PTCP as it enables the nanofluid to absorb more solar energy. Enhancing the collector length accelerates the thermal loss to the ambient, as a result the system performance diminishes. It is also regarded that the heat absorption of the nanofluid declines with improving inlet temperature of the working fluid.

1. Introduction

Solar energy is one of the most important sources of non-conventional energy because of its clean, widespread, and abundant properties [1]. Given the today's increasing energy use and demand, it can be regarded as one of the best natural resources in terms of protecting the environment and preventing energy deficiency among renewable energy sources [2]. However, for this, solar radiation must be captured and converted into thermal energy via a solar collector. In a surface-based solar collector (SBSC), solar irradiation is absorbed through an absorber surface and then transferred to heat transfer fluid via conduction and convection heat transfer from the absorber. Hence, the PTCP of the collector is adversely altered by the increased thermal loss between the working fluid and absorber. A direct absorption solar collector (DASC) is used [3,4] to diminish the thermal loss and enhance the PTCE of the collector. In that, solar irradiance was directly absorbed by the fluid, resulted in the enhanced PTCE compared to a SBSC [5,6].

However, the most important factor that impacts the PTCP of DASCs is the optical and thermal characteristics of heat transfer fluid such as density or attenuation capacity [7,8]. Because a conventional working fluid has a low absorptivity to absorb solar irradiation, the PTCE is low. When water is compared to other base fluids such as ethylene glycol, and Therminol VP-1, although it ranks as the best absorber, it absorbs just 13 % of solar energy [9]. However, with the development of nanotechnology, by adding nanoparticles to a host fluid, the heat transfer fluid's optical performance is improved [10]. Besides, nanofluids increase the heat transfer process because of their high surface area and thermal conductivity. Cao *et al.* [11] experimentally scrutinized the radiative properties of ionic liquid-based nanofluids. The results showed that the absorption properties of working fluid diminished with increasing cation or anion radius and were affected by high viscosity. They also found that the absorption efficiency and extinction coefficients have the same trend. Karami *et al.* [12] experimentally analysed the characteristics of carbon nanoballs (CNBs)/water and CNBs/ethylene glycol nanofluids. They found that, on average, the extinction coefficient of ethylene glycol and water was increased by 3.4 1 cm^{-1} and 3.9 1 cm^{-1}, respectively with an addition of 300 ppm CNBs. Gan and Qiao [13] experimentally evaluated the radiative heat transfer and optical properties of carbon-based nanofluids in the UV–vis range. The findings showed that multiwalled carbon nanotubes (MWCNTs)/ethanol-based or carbon nanoparticles (CNPs)/ethanol-based nanofluids

* Corresponding author.
E-mail address: Manosh.Paul@glasgow.ac.uk (M.C. Paul).

https://doi.org/10.1016/j.molliq.2024.125702
Received 11 April 2024; Received in revised form 31 July 2024; Accepted 3 August 2024
Available online 5 August 2024

Nomenclature

$\dot{Q}_{usefulheat}$	Useful heat (W)
L	Collector length (m)
$\vec{r}$	Position vector
U	Fluid velocity (m/s)
I_λ	Radiation intensity (W/m^{2}μm)
$PTCE$	Photo-thermal conversion efficiency
m	Normalized refractive index of the particle to the fluid
T	Temperature
FVM	Finite volume method
$I_{b\lambda}$	Black body intensity (W/m^{2}μm)
$\vec{s}$	Direction vector
E	Enhancement
$PTCP$	Photo-thermal conversion performance
$K_{a\lambda}$	Absorption coefficient (1/m)
C_p	Specific heat (J/kgK)
$Q_{a\lambda}$	Absorption efficiency
NVC	Nanoparticle volume concentration
$K_{s\lambda}$	Scattering coefficient (1/m)
α	Size parameter
RTE	Radiative transport equation
k	Thermal conductivity (W/mK)
w	Wind speed (5 m/s)
G	Solar density (W/m^2)
$Q_{s\lambda}$	Scattering efficiency
n	Refractive index
$\dot{m}$	Mass flow rate (kg/s)
D	Particle diameter (m)
$\vec{s}'$	Scattering direction vector
L/H	Aspect ratio
$K_{e\lambda}$	Extinction coefficient (1/m)
$VHSC$	Volumetrically heated solar collector
$Q_{e\lambda}$	Extinction efficiency
p	Pressure (Pa)
A	Top surface area (m^2)
u, v	Velocity vectors (m/s)
H	Collector height (m)
h	Convective heat transfer coefficient (W/m^{2}K)
ΔT	Temperature difference
f_v	Particle volume fraction

Greek symbols

Φ	Phase function
λ	Wavelength of incident light (μm)
ε	Emissivity (0.95)
σ	Stefan Boltzmann(5.67×10^{-8} W/m^{2}K^4)
Ω'	Solid angle
μ	Dynamic viscosity (Ns/m^2)
ρ	Density (kg/m^3)

Subscripts

r	Radiative
in	Inlet
amb	Ambient
out	Outlet
nf	Nanofluid

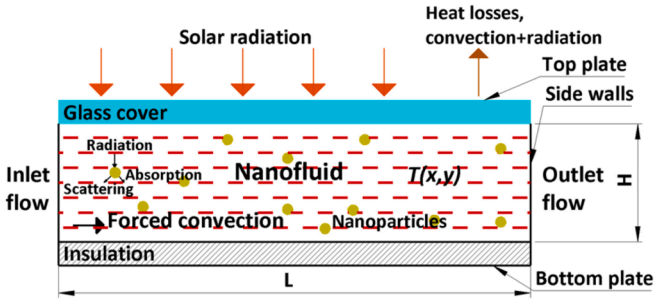

Fig. 1. The schematic of a 2D DASC.

Table 1
Thermophysical properties of nanoparticles [30,31,32,33].

Properties	Ag	MgO	Graphite	TiO_2
k(W/mK)	429	45	1950	8.9538
ρ(kg/m^3)	10,500	3560	2210	4250
C_p(J/kgK)	235	955	709	686.2

have higher evaporation ratio than pure ethanol. In addition, MWCNTs/ethanol-based nanofluids had a higher droplet temperature when compared to CNPs or aluminium (Al) nanoparticles. They used the Rayleigh approach to measure optical properties, and MWCNTs were found to have the best nanoparticles for radiation absorption.

Qin *et al.* [14] researched the absorption performance of plasmonic nanofluids with different nanoparticle shapes. The numerical results indicated that the thermal capacity of tetrahedral nanoparticle at a constant volume fraction of 1 ppm is 20 % and 35 % than nanorod and nanosphere, respectively. The lightning rod effect could also be enhanced by the sharper edges. Gimeno-Furió *et al.* [15] experimentally analysed the impacts of low carbon NVCs (3 and 33 ml/g) on the optical properties and PTCP in a low temperature DASC. Carbon nanoparticles added at high volume NPV enhanced the absorption coefficient of pure water by 3200 %. It was found that the temperature of water, low and high concentration nanofluids attains at 9.3 °C, 20 °C and 24.2 °C, respectively at the end of a radiation period of 6000 s. Wang *et al.* [16] investigated MXene and graphene nanofluids with different NVCs of 5, 10, 20, 40, 60 ppm in application of DASC. The experimental results indicated that MXene nanofluid has better PTCP at the same NVC of 20 ppm as 63.35 %. It was also found that as the NVC and temperature increase, the thermal conductivity of these nanofluids enhance. Zhu *et al.* [17] demonstrated the usage of ZIF-8-derived N-doped graphitic polyhedrons (ZNGs) as carbon matrix, Ag-Au/ZNGs nanocomposites with different weight fractions of 10, 30, 50, 70, 100 ppm for the

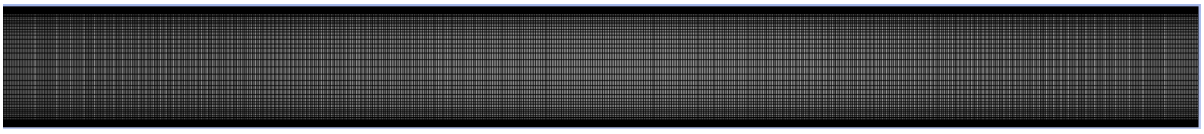

Fig. 2. Mesh generation inside the DASC.

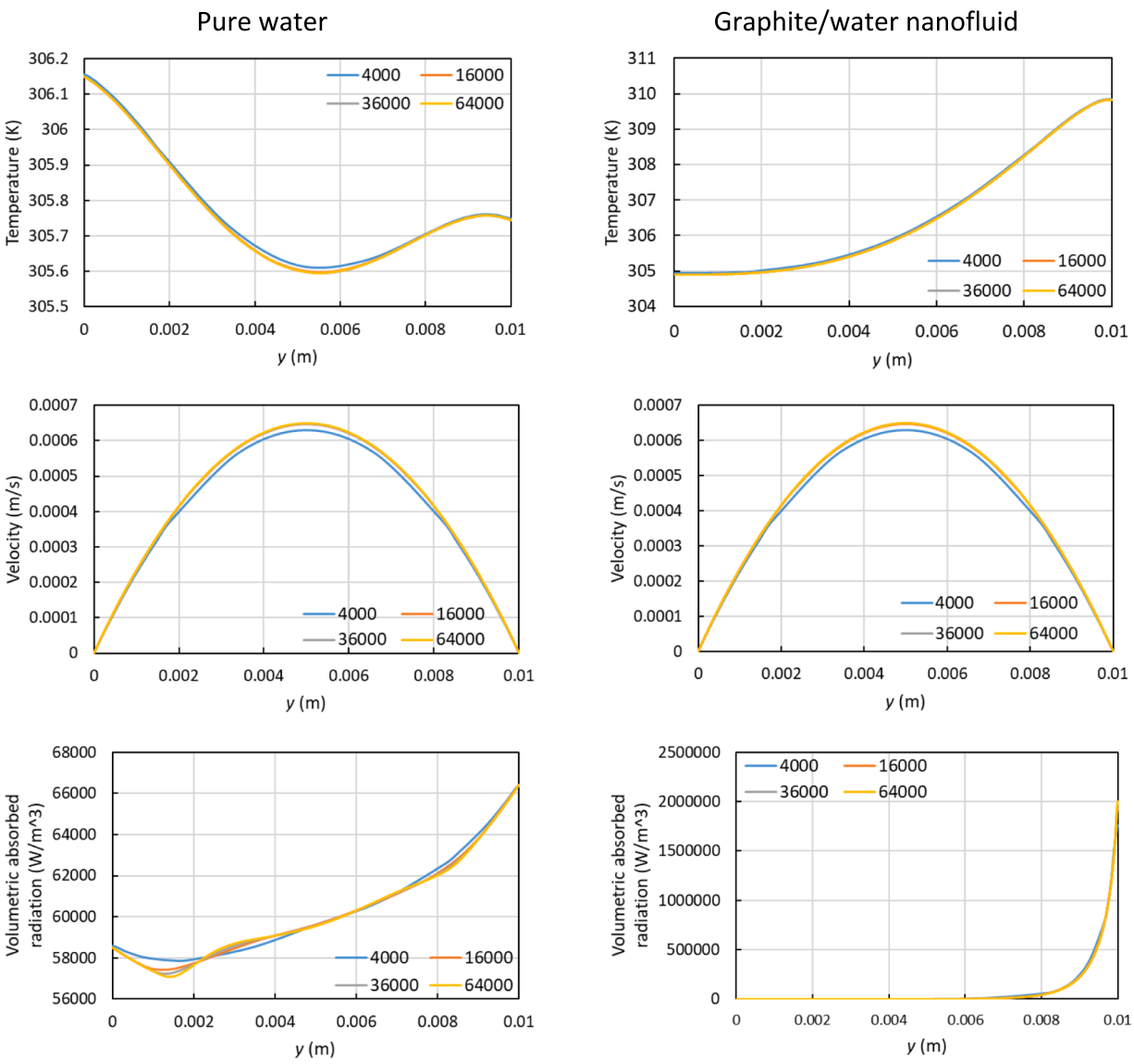

Fig. 3. Variations of temperature, velocity, and volumetric absorbed radiation with different grid numbers of 4000, 16000, 36000, 64,000 using pure water (left) and Graphite/water nanofluid (right).

application of solar energy. The experimental results further revealed that Ag-Au/ZNGs, monometallic ZNGs nanofluids and ZNGs nanofluids have better thermal performance than pure ethylene glycol. The thermal performance of Ag-Au/ZNGs nanofluids was 5 % and 36 % higher than ZNGs ethylene glycol nanofluid and pure ethylene glycol, respectively.

In addition to the nanoparticles' optical properties and absorption characteristics, the flow rate of the fluid flowing in solar collectors is another factor that affects the PTCP by changing the fluid's exit temperature. Gupta *et al.* [18] analysed the PTCP of DASC using water based Al_2O_3 nanofluid of various NVCs (0.001 %, 0.005 %, 0.01 % and 0.02 %) with a diameter of 20 nm. Their experimental findings revealed that the PTCE was augmented by using nanofluids. Especially, the augmentation of PTCE was found to be 32.3 % and 12.8 % for 10 and 100 ppm, respectively, although it was discovered that the PTCE was negatively affected by NVCs. Thakur *et al.* [19] implemented experimental research in a microchannel-based DASC using silica/fly ash and alumina/fly ash nanofluids. The results revealed that the PTCE was 59.23 % and 72.82 % for silica/fly ash and alumina/fly ash nanofluids, respectively. It was also found that the exergy efficiency is 68.09 % and 73 % and for silica/fly ash and alumina/fly ash nanofluids, respectively. Vakili *et al.* [20] explored the PTCP of VHSC using graphene/deionized water nanofluid with weight concentrations of 0.05 %, 0.1 % and 0.5 % at various mass flow rates and inlet temperatures. Their experimental findings discovered that nanoparticle addiction enhanced the collector's PTCP, and the "zero-loss" efficiencies were 83.5 %, 89.7 % and 93.2 % with concentrations of 0.05 %, 0.1 % and 0.5 %, respectively.

1.1. Contributions of this study

As mentioned by the literature review, nanoparticles have the capability to augment both the thermal and optical characteristics of the host fluid. Most studies show that absorption and thermal performances of mono nanofluids are examined under motionless conditions, however, the working fluid's velocity is a critical element that could affect the PTCE. Especially when the change of a collector length combined with the working fluid's thermal abilities is influenced by the working factors like temperature, it is currently unknown how these changing conditions affect the overall thermal/optical performance of hybrid nanofluid.

Moreover, there is still a lack of information and clear knowledge gap

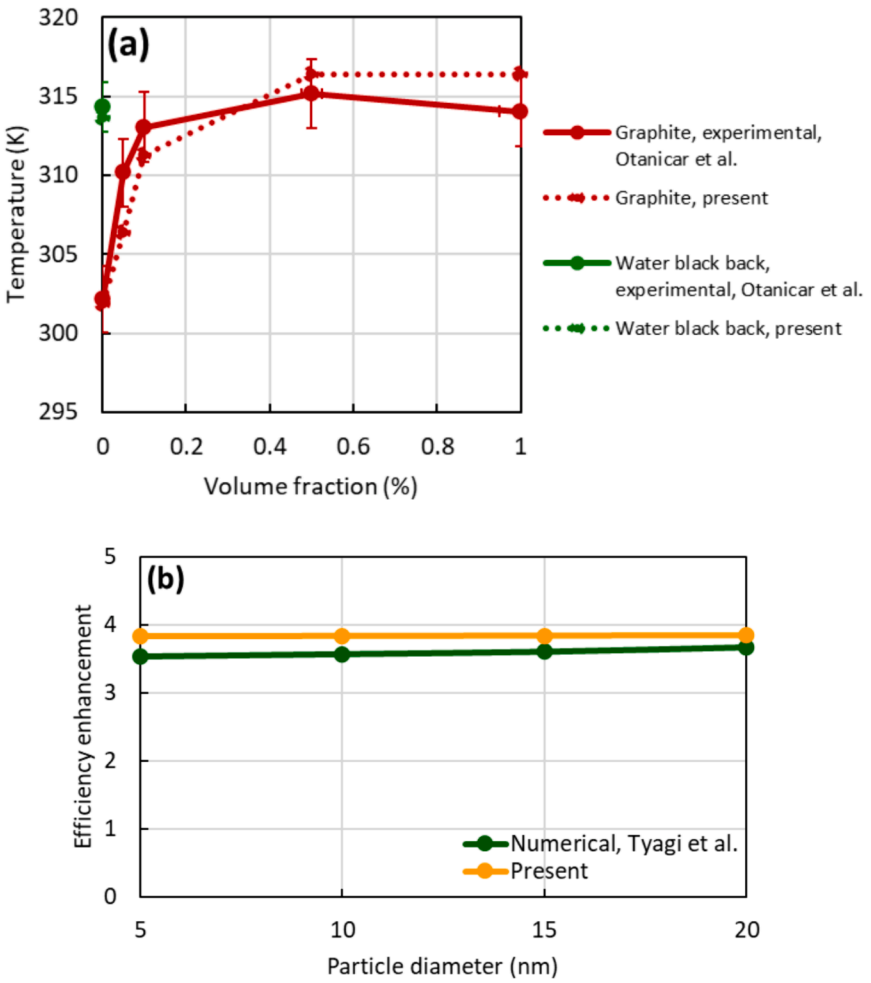

Fig. 4. Comparison of the collector performance vs. particle concentration (a) and particle size (b) results between the present study and the benchmark cases [35,5].

in the published literatures about the choice of hybrid particles and influence they would have on the optical characteristics. Interaction of radiation with hybrid particles, therefore, needs to be understood.

Furthermore, the NVC is another important factor that could affect the flow, optical and thermal abilities of heat transfer fluid. It is also currently unknown how the PTCP of nanoparticles prepared at a low NVC will affect a collector when the high NVC is employed.

Last but not the least, the major contribution of the current investigation is that the combined impacts of volumetric absorption and thermal radiation on the PTCP under these research gaps, as well as the impacts on collector's length, nanoparticle size and operating temperature, still needs to be investigated due to the lack of information in the published studies. Due to the inadequate understanding of the effects of these coupled impacts on the fluid-flow physics, this is another point that needs to be examined. In light of this, the target of this investigation is to focus on the examination of the effects of coupled convection and radiation heat transfer and flow on the nanoparticle-based photothermal capacity by applying a comprehensive numerical method. It is also of special importance to elucidate for the first-time the influence of MgO nanoparticles in a VHSC.

2. Modelling and methodology

As illustrated in Fig. 1, a 2D fluid flow and heat transfer model is established and resolved numerically to evaluate the PTCP of a DASC having the L/H of 10 [21]. As the sunbeam penetrates the solar collector vertically, the upper plate of the is enveloped with a translucent glass coating, enabling most sunlight to be absorbed by the nanofluid. Any ambient thermal loss occurs through combined radiation and convection.

The RTE is carried out to interpret the irradiation's spectral attenuation inside the translucent flow status, and is characterized as [22]:

$$\nabla \bullet (I_\lambda(\vec{r}, \vec{s})\vec{s}) + (K_{a\lambda} + K_{s\lambda})I_\lambda(\vec{r}, \vec{s}) = K_{a\lambda}n^2 I_{b\lambda} + \frac{K_{s\lambda}}{4\pi}\int_0^{4\pi} I_\lambda(\vec{r}, \vec{s}')\Phi(\vec{s} \bullet \vec{s}')d\Omega' \quad (1)$$

Due to the absorption's domination towards attenuation, scattering impacts can be disregarded in water as a pure liquid, thus the extinction coefficient can be determined as [5]:

$$K_{e\lambda,f} = K_{a\lambda,f} = \frac{4\pi k}{\lambda} \quad (2)$$

The Rayleigh scattering can contribute to the calculation of the nanoparticles' optical characteristics [23] since particle size or NVC alters the nanofluids' scattering or absorption characteristics. The extinction coefficient, hence, can be presented as [5]:

$$K_{e\lambda,p} = \frac{3f_v Q_{e\lambda}(\alpha, m)}{D} \quad (3)$$

where α and m can be identified as [5]:

$$m = \frac{m_{particles}}{n_{fluid}} \quad (4)$$

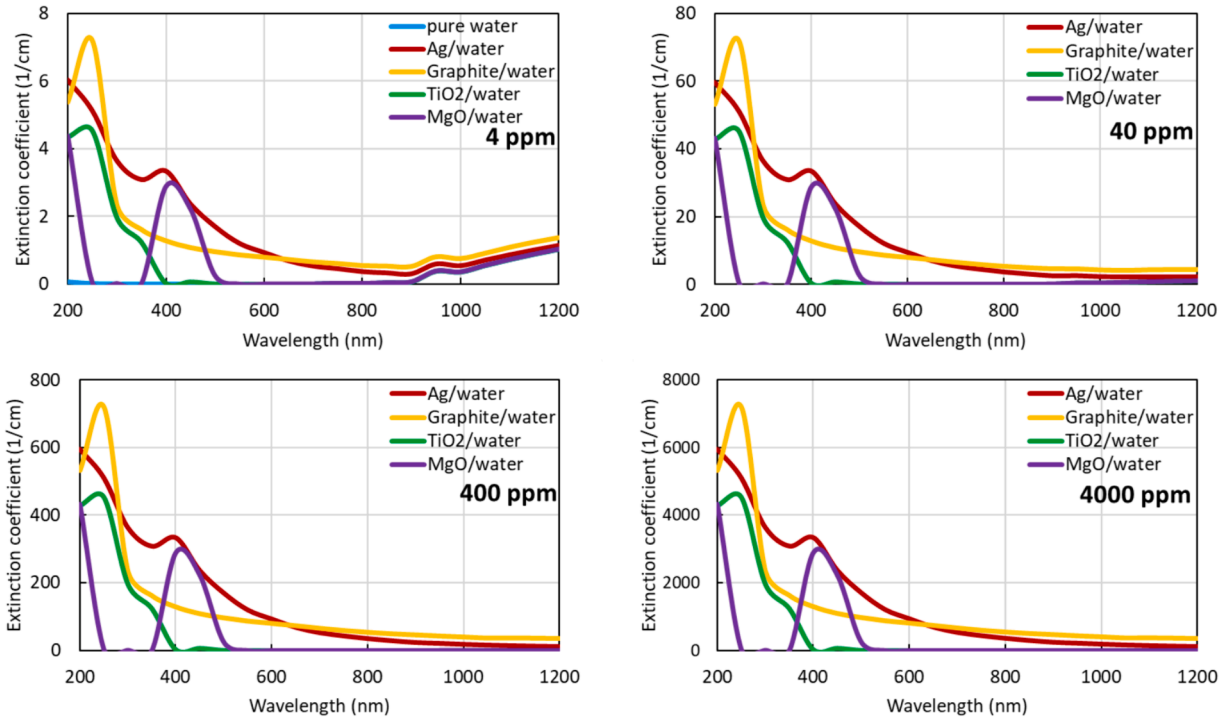

Fig. 5. Impact of NVC on the optical behaviours of nanofluids.

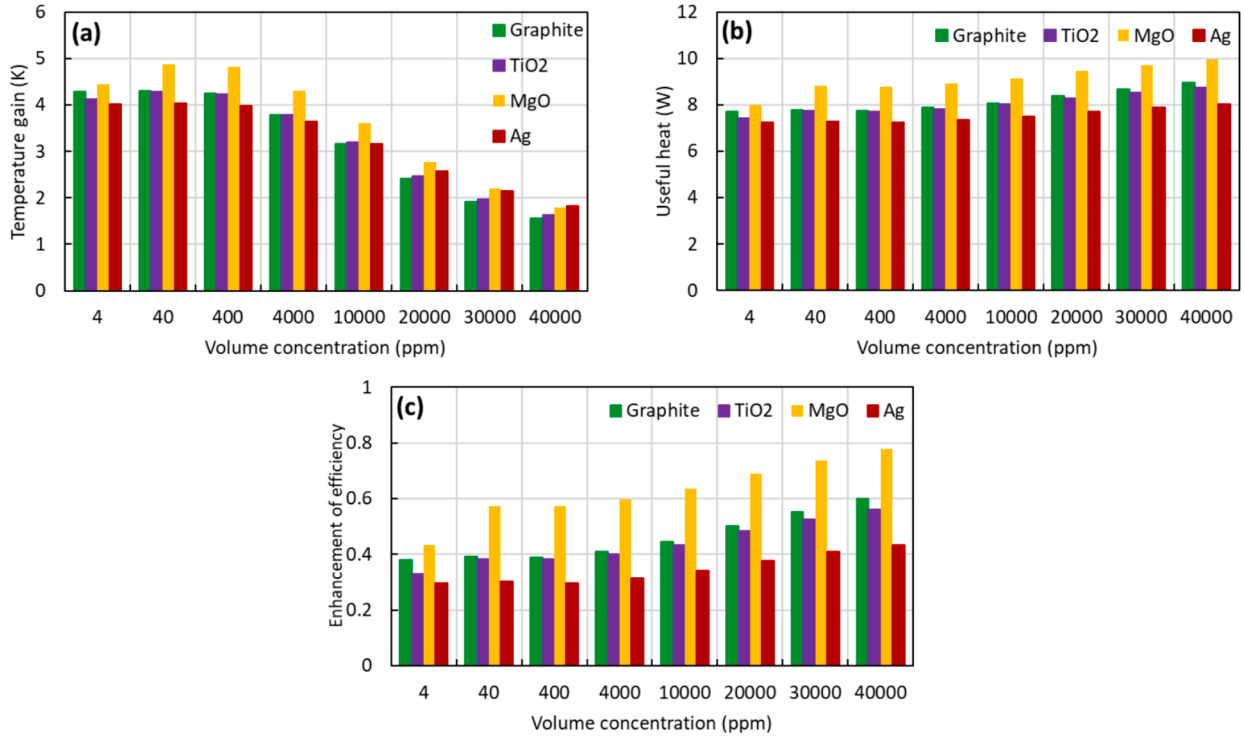

Fig. 6. Impact of various nanoparticles on the PTCP: (a) temperature rise, (b) heat gain, (c) enhancement of efficiency with varying NVCs.

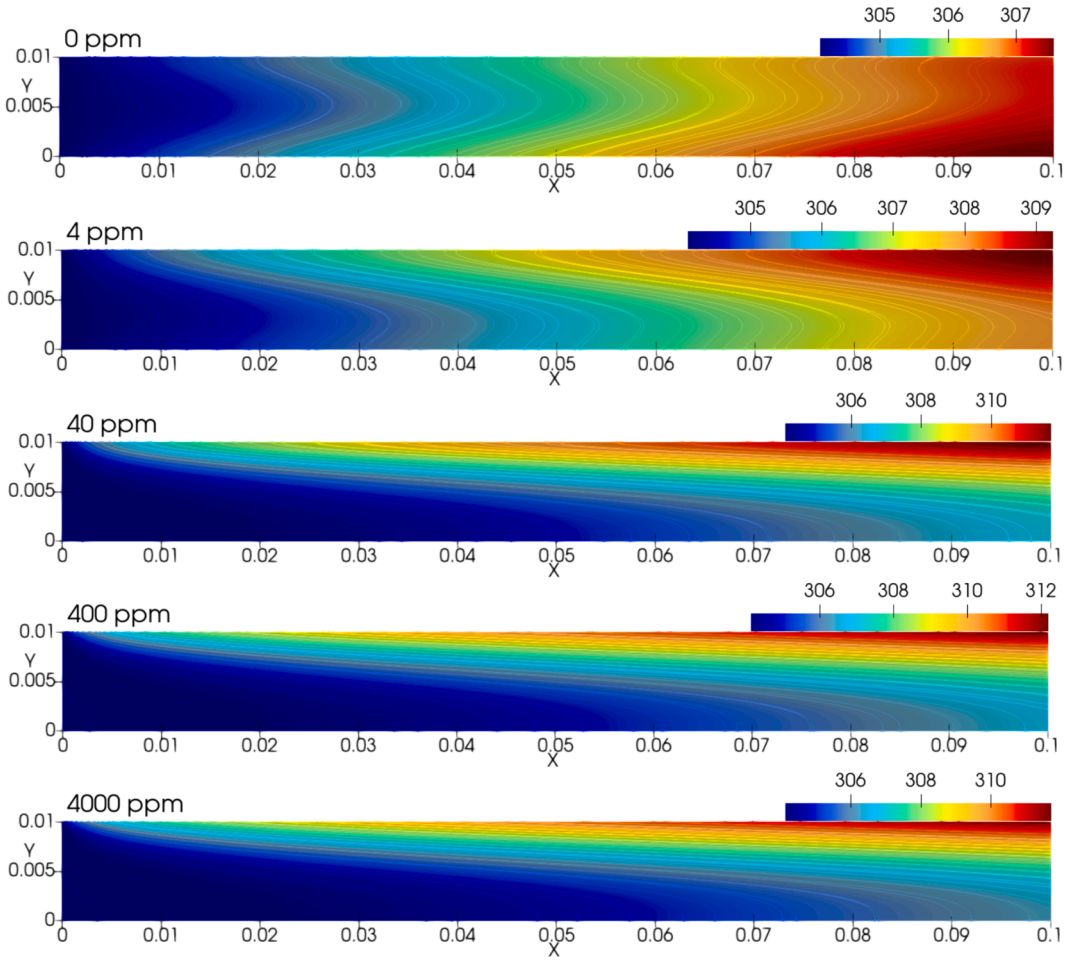

Fig. 7. Temperature (K) profiles of graphite nanofluids at various NVCs.

$$m_{particles} = n + ik \tag{5}$$

$$\alpha = \frac{\pi D}{\lambda} \tag{6}$$

where k is the absorption index. The nanoparticles and water' optical properties were also obtained from literature [24,25,26] so that the efficiency of extinction is calculated as [23]:

$$Q_{e\lambda} = Q_{a\lambda} + Q_{s\lambda} \tag{7}$$

where

$$Q_{s\lambda} = \frac{8}{3}\alpha^4 \left| \left(\frac{m^2 - 1}{m^2 + 2} \right) \right|^2 \tag{8}$$

$$Q_{a\lambda} = 4\alpha Im\left\{ \frac{m^2 - 1}{m^2 + 2} \left[1 + \frac{\alpha^2}{15} \left(\frac{m^2 - 1}{m^2 + 2} \right) \frac{m^4 + 27m^2 + 38}{2m^2 + 3} \right] \right\} \tag{9}$$

The sum of the extinction or attenuation coefficient of nanoparticles and host fluid, therefore, is equal to the nanofluid's effective extinction coefficient as:

$$K_{e\lambda,nf} = K_{e\lambda,p} + K_{e\lambda,f} \tag{10}$$

The nanofluid flow inside the VHSC is assumed to be steady state, incompressible, Newtonian, and laminar. The nanoparticles of the identical size and spherical shape are in thermal balance and in the equal velocity with the fluid phase. The governing equations are also given as:

$$\frac{\partial u}{\partial x} + \frac{\partial v}{\partial y} = 0 \tag{11}$$

$$u\frac{\partial u}{\partial x} + v\frac{\partial u}{\partial y} = -\frac{1}{\rho_{nf}}\frac{\partial p}{\partial x} + \frac{\mu_{nf}}{\rho_{nf}}\left(\frac{\partial^2 u}{\partial x^2} + \frac{\partial^2 u}{\partial y^2} \right) \tag{12}$$

$$u\frac{\partial v}{\partial x} + v\frac{\partial v}{\partial y} = -\frac{1}{\rho_{nf}}\frac{\partial p}{\partial y} + \frac{\mu_{nf}}{\rho_{nf}}\left(\frac{\partial^2 v}{\partial x^2} + \frac{\partial^2 v}{\partial y^2} \right) \tag{13}$$

$$\rho_{nf} c_{p_{nf}} \left(u\frac{\partial T}{\partial x} + v\frac{\partial T}{\partial y} \right) = k_{nf}\left(\frac{\partial^2 T}{\partial x^2} + \frac{\partial^2 T}{\partial y^2} \right) - \frac{\partial q_r}{\partial y} \tag{14}$$

The boundary conditions of the system, correspondingly, are:
At the surface of plates:

$$u = v = 0 \tag{15}$$

At the bottom:

$$\frac{\partial T}{\partial y} = 0 \tag{16}$$

At the outlet:

$$p = 0 \tag{17}$$

At the inlet:

$$u = U_{in}, T = T_{in}, v = 0 \tag{18}$$

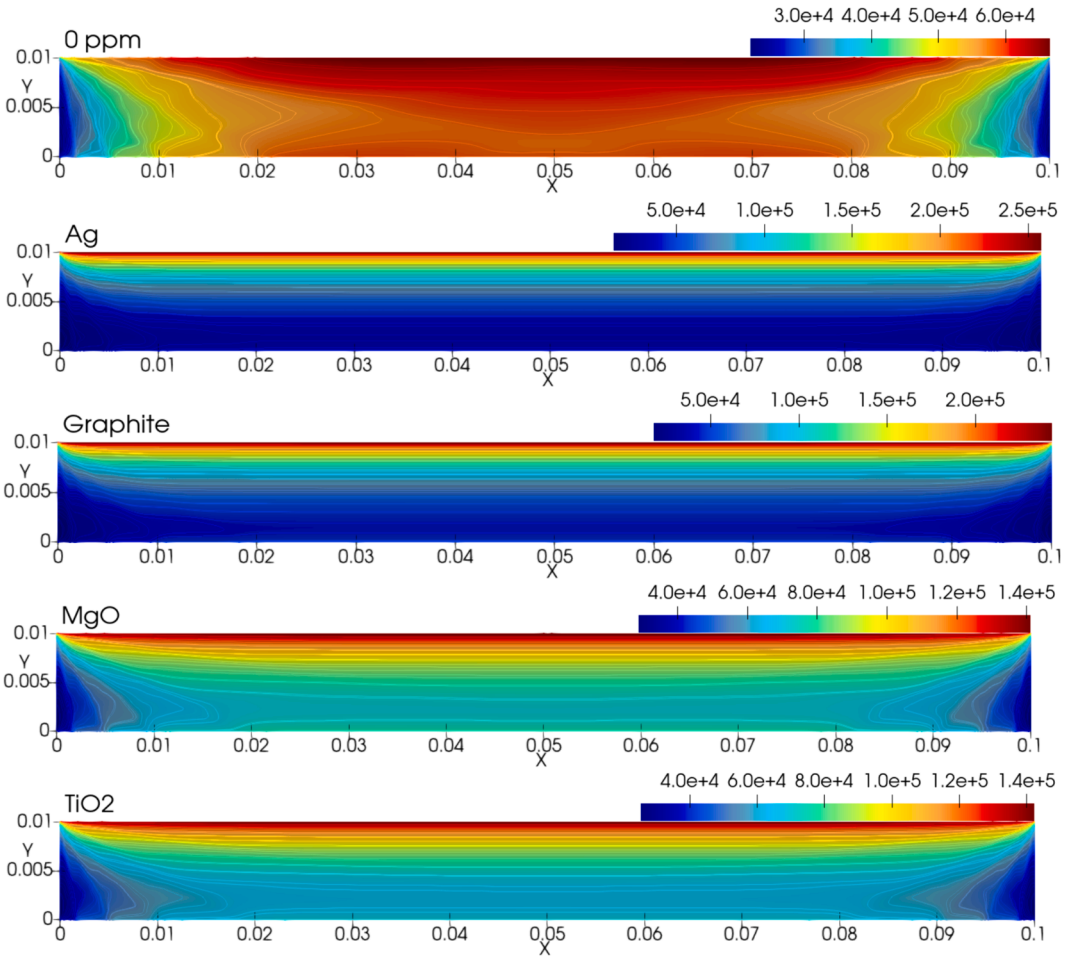

Fig. 8. Volumetric absorbed radiation (Wm^{-3}) profiles of various mono nanofluids for a NVC of 4 ppm.

At the upper layer panel:

$$q = h(T - T_{amb}) + \varepsilon\sigma(T^4 - T_{amb}^4) \tag{19}$$

where h is described as [27]:

$$h = 5.7 + 3.8w \tag{20}$$

Moreover, details about the modelling of mono and blended nanofluids thermophysical properties were already described in the authors' previous examinations [28,29]. Further, the nanoparticles' thermophysical properties are given in Table 1.

The PTCE can be defined by [34]:

$$\eta = \frac{\dot{m}C_p(T_{out} - T_{in})}{AG} = \frac{\rho HUC_p(T_{out} - T_{in})}{LG} \tag{21}$$

The heat generation throughout the photothermal conversion process is computed by:

$$\dot{Q}_{usefulheat} = \dot{m}c_p\Delta T \tag{22}$$

Finally, enhancement of PTCE of nanofluid in DASC when compared to the pure water, is expressed as:

$$E = \frac{thermalvariable_{nanofluid} - thermalvariable_{water}}{thermalvariable_{water}} \tag{23}$$

where the *thermal variable* represents the efficiency.

The numerical procedure which is the pressure based FVM utilized to resolve the governing equations was detailed in the authors' earlier investigations by applying ANSYS Fluent 2020 R1 [28,29]. The method of Discrete Ordinates (DO) was also employed for solving the RTE including emitting, scattering, and absorbing aspects. The energy and DO' residuals are also remained under 10^{-6} while for the other equations are below 10^{-5} to get more uniform and reliable results.

3. Model validation and grid sensitivity

3.1. Mesh dependency test

A grid independence checking is implemented to obtain the resolutions which are independent to the grid quantities chosen. Fig. 2 presents the physical domain created by non-uniform grid. The results of the grid independence test are displayed in Fig. 3, showing the variation of temperature, velocity, and volumetric absorbed radiation with different grid sizes which are 4000, 16000, 36000, 64,000 using pure water and Graphite/water nanofluid. As demonstrated in Fig. 3, the computational results beyond the chosen mesh numbers of 16,000 do not vary and therefore one of the three higher resolution grids can be taken to proceed the simulations. In order to minimise the computational time, the mesh numbers of 16,000 is therefore selected for the further calculations.

3.2. Model validation

The current numerical modelling prediction is compared with the experimental and modelling results in the published papers ([5,35]). Hereby, the study of Otanicar et al. [35] is selected for the first validation of the computational results of the PTCP of the DASC using Graphite

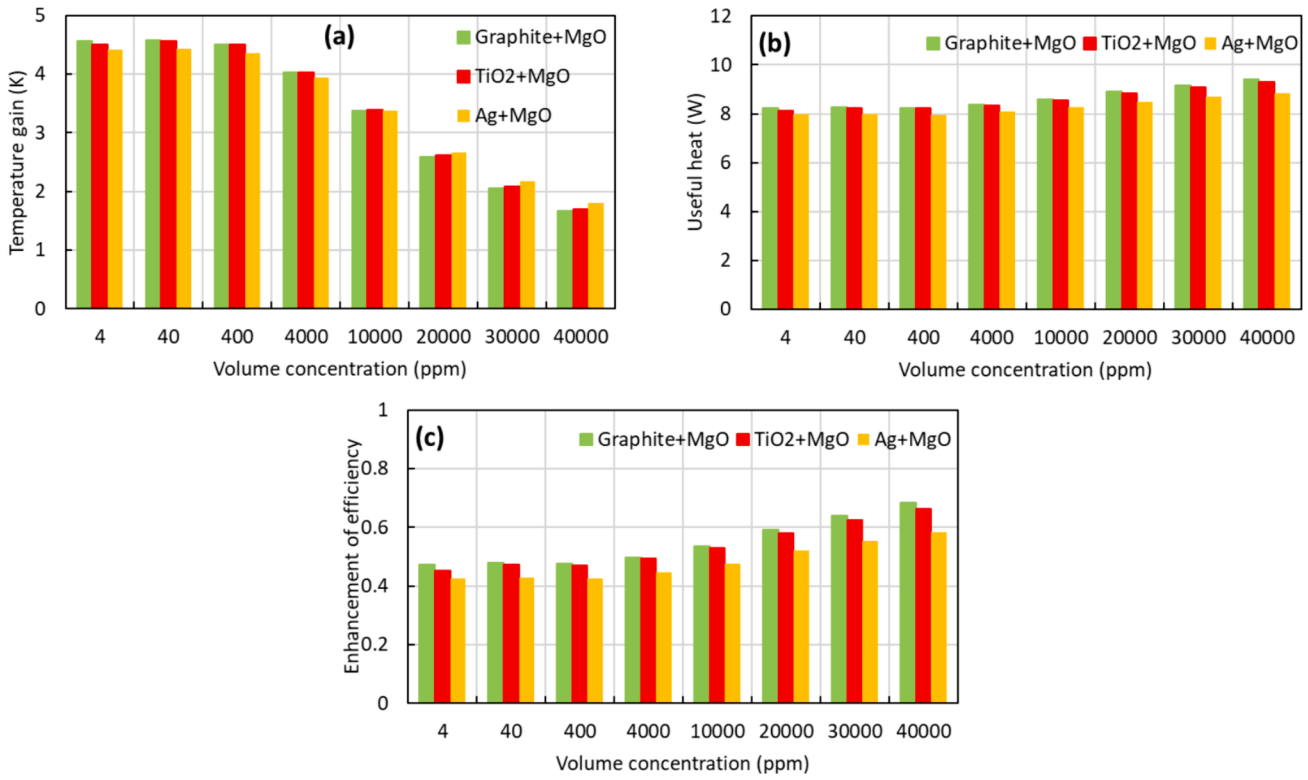

Fig. 9. Impact of various nanoparticles on the PTCP (a) temperature rise, (b) heat gain, (c) enhancement of efficiency with varying NVCs.

nanoparticles and different NVCs. A flow rate of 42 ml/h for the nanofluid is used in the DASC and the solar irradiation penetrates at 1000 Wm^{-2} while the thermal loss occurring by combined radiation and convection is measured at $h = 23\,Wm^{-2}K^{-1}$. As distinguished in Fig. 4a, the maximum error is 1.23 %, and the present results match well with the data set [35]. The second validation is performed against the results of Tyagi et al. [5] in which the PTCE of the DASC is presented for Al/water nanofluid with different nanoparticle diameters. The upper surface is exposed to irradiance at 1000 Wm^{-2} and thermal losses by convection, $h = 6\,Wm^{-2}K^{-1}$ while the bottom wall is kept adiabatic. As presented in Fig. 4b, the maximum error is 8.34 %, and thus the present collector efficiency is also in good agreement with the second benchmark model [5].

4. Results and discussion

This section initially highlights the nanofluids' optical characteristics, followed by the influences of the nanoparticle type and NVC, Reynolds number, particle size, operating temperature, and collector structure on the PTCP.

4.1. Optical properties of nanofluids

The fluids' optical characteristics depend on the scattering and absorption coefficients. Since absorption in pure water dominates attenuation, scattering effects in pure water can be neglected. As seen in Fig. 5 (4 ppm), the pure water's attenuation coefficient depends on the absorption coefficient. Water is deemed as a semi-transparent media at solar spectra wavelengths in the range of 200–1200 nm, and water turns into an effective absorber once solar radiation spectrum switches to near-infrared region [36]. Nanoparticle addition to the pure water can augment more absorption in these ranges since energy's 85 % of the sun's rays reaches the earth's thick outer shell of rock in these solar spectra range [37]. As indicated in Fig. 5, by adding different nanoparticles to pure water, the solar irradiance absorption power of the fluid augments. Since various particles have dissimilar optical features, their effects in the extinction coefficients and wavelength ranges are different. While the peak point of Graphite/water and TiO_2/water nanofluids is at 250 nm wavelength, the peak point of Ag/water and MgO/water nanofluids occurs at 200 nm wavelength. Even at low NVCs (e.g. 4 ppm), nanoparticles added to water significantly improve the attenuation coefficient in the ultraviolet and visible light spectrum. From low NVCs to high NVCs, the light's absorption enhances by increasing the absorption coefficient of nanofluids. This augmentation by NVC is in accord with the point of view of Karami *et al.* [12]. Moreover, since the hybrid nanofluids' attenuation coefficient is the total of nanoparticles' attenuation coefficient that make up the nanofluid, their extinction coefficient is higher than the mono nanofluids. It is endorsed by the exploration of Rabbi et al. [38].

4.2. Combined impacts of nanoparticle type and particle concentration

The impacts of mono nanoparticle type are analysed using Graphite, TiO_2, MgO and Ag nanoparticles with changing from low NVCs (4–4000 ppm) to high NVCs (10000–40000 ppm). The power of nanofluid to absorb sun rays depends on the extinction coefficient. Since the enhancement in the NVC improves the absorption capacity of the nanofluid due to radiation-nanoparticle interaction, the working fluid absorbs more solar energy. In addition, because the fluid's flow rate changes with the changing NVC, the collector's performance is affected differently. Although the nanofluid's temperature rise boosts slowly, especially in the NVC range of 4–400 ppm (Fig. 6(a)), it is better than that of water (3.1 K). After 400 ppm, as the fluid's flow rate improves faster, the nanofluid accelerates more. Hence, the temperature gain decreases as the solar irradiation absorption time of the nanofluid declines throughout the collector. Despite this reduction in temperature, the augmentation in the flow rate with the enhancement in the NVC enhances the rate of usable thermal energy of nanofluid compared to base fluid (5.59 W), as demonstrated in Fig. 6(b). Thus, the collector efficiency improves as in Fig. 6(c). Furthermore, because the nanofluid is

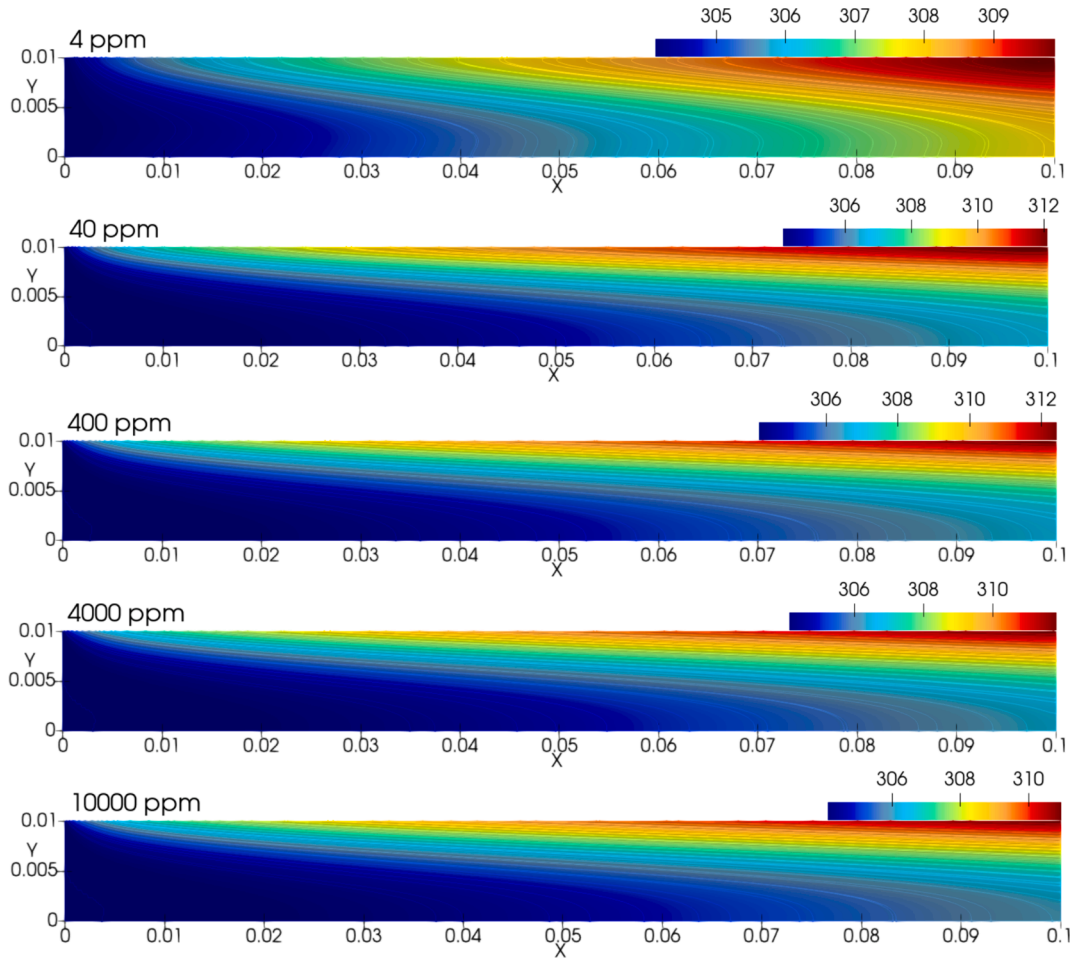

Fig. 10. Temperature (K) profiles of Ag + MgO nanofluids at various NVCs.

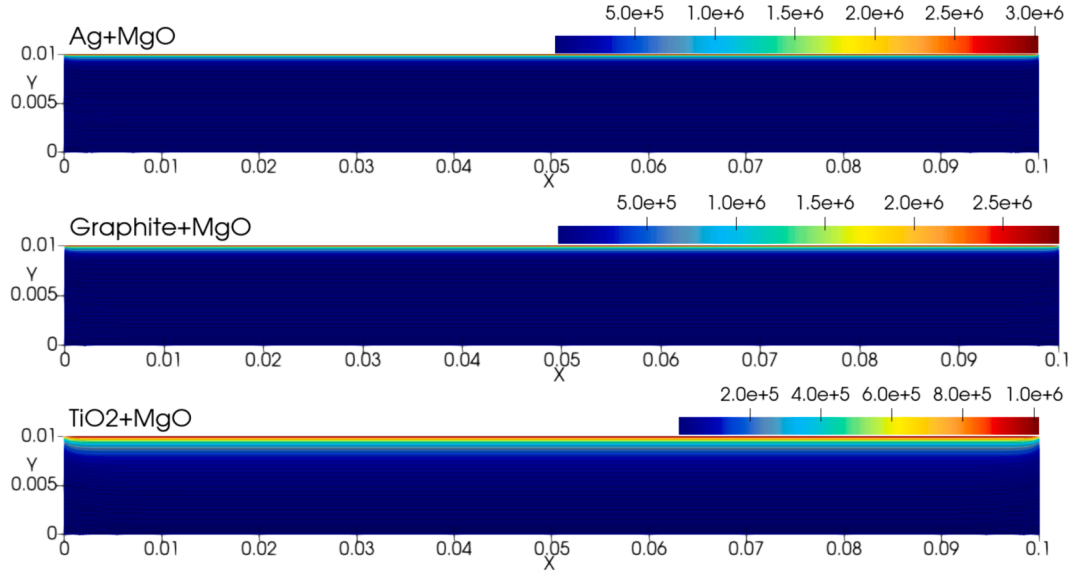

Fig. 11. Volumetric absorbed radiation (Wm^{-3}) profiles of various hybrid nanofluids for NVC of 40 ppm.

utilized simultaneously as a storage medium and an operating fluid in a DASC, the particle addition to the water therefore enhances the storage capability by improving the solar thermal capture. The current performance enhancement with increasing NVC is supported by the idea of Vakili *et al.* [20].

Moreover, the temperature distribution inside the DASC of water-based graphite nanofluid at various NVCs is seen in Fig. 7. In the absence of nanoparticle effect (0 ppm), solar radiation reaches the base

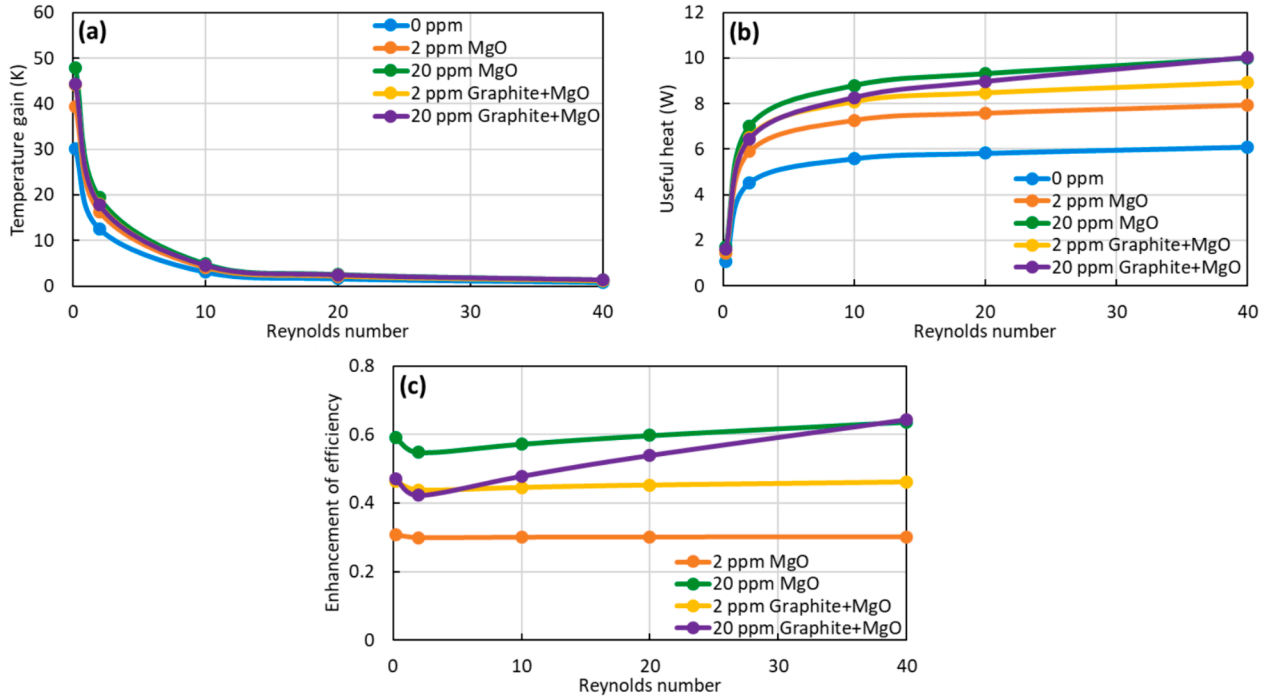

Fig. 12. Impact of Reynolds number on the PTCP (a) temperature rise, (b) heat gain, (c) enhancement of efficiency with varying Reynolds number.

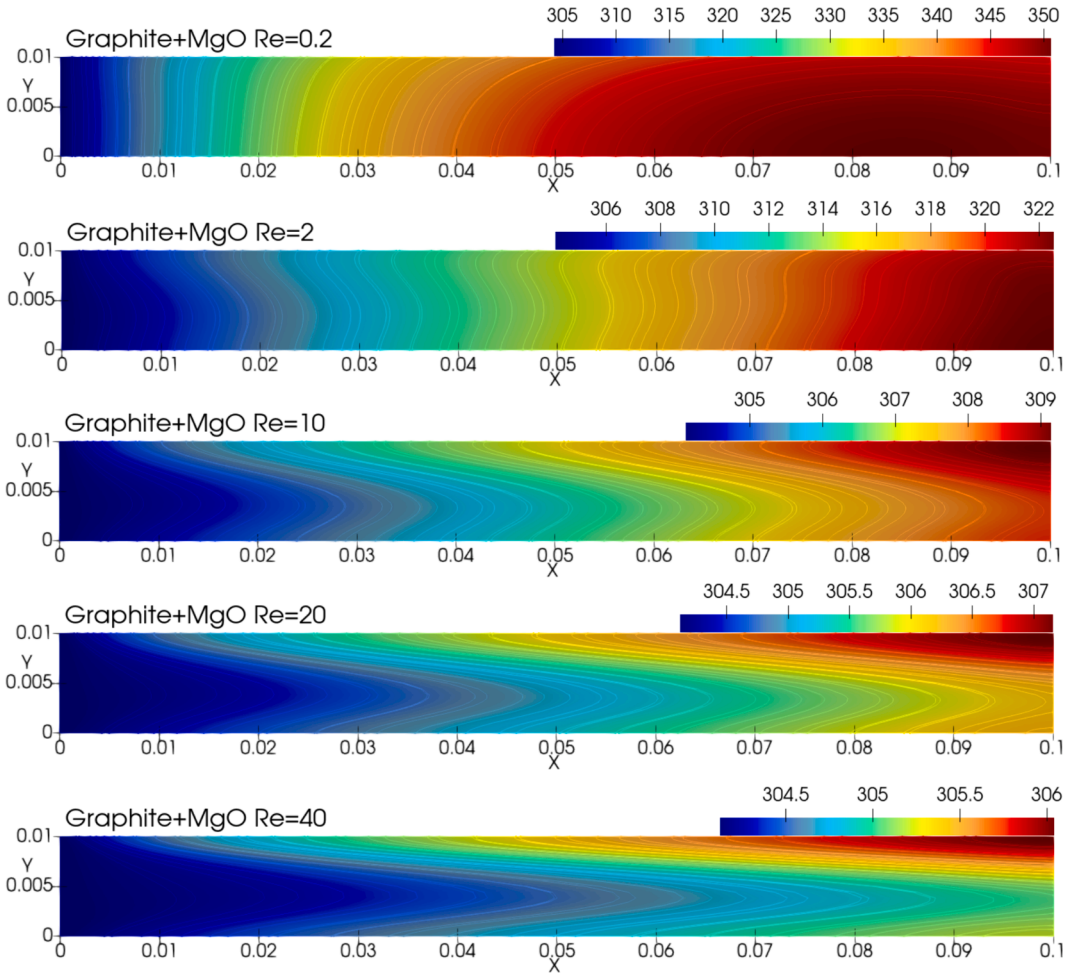

Fig. 13. Temperature (Kelvin, K) profiles of nanofluids with varying Reynolds number at NVC of 2 ppm.

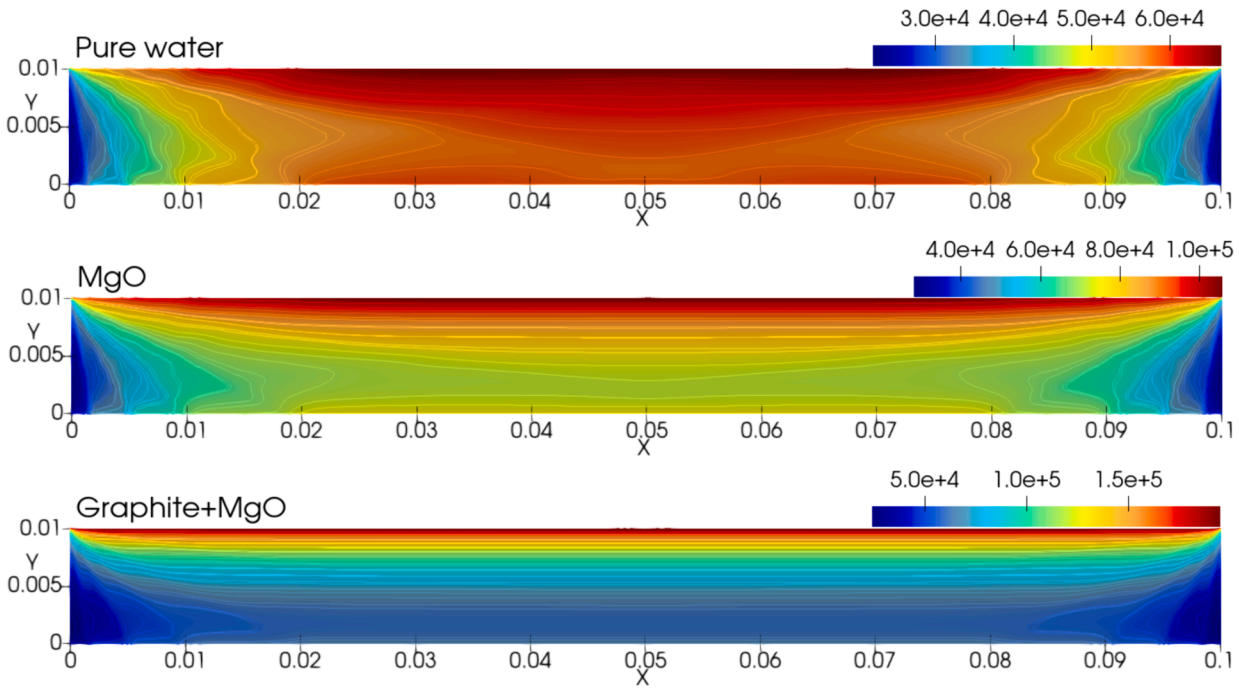

Fig. 14. Volumetric absorbed radiation (Wm^{-3}) profiles at NVC of 2 ppm.

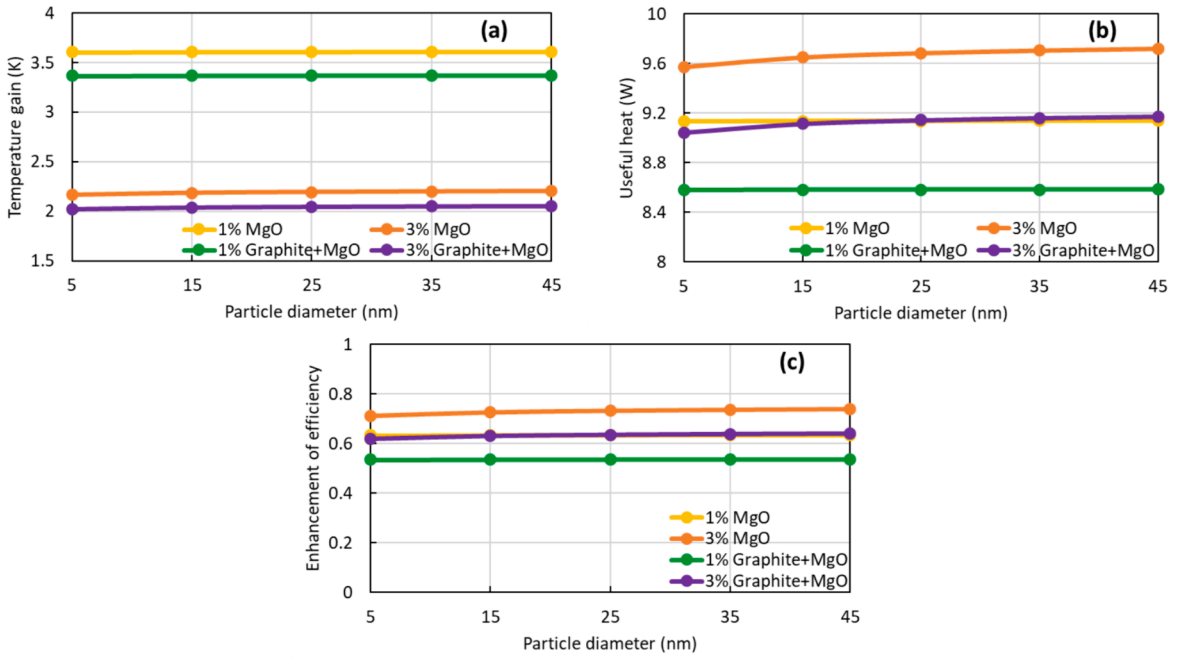

Fig. 15. Impact of nanoparticle size on the PTCP (a) temperature rise, (b) heat gain, (c) enhancement of efficiency with varying particle diameter.

plate of the collector and is absorbed by the fluid layer at the vicinity of the bottom panel, providing a more uniform temperature propagation within the collector. With the addition of the nanoparticle, however, the effect of sunlight decreases with the depth of the fluid, so the radiation cannot penetrate too much into the lower layers of the collector. Therefore, the radiation is absorbed by the fluid layers close to the upper layers of the collector, and the temperature variation inside the collector raises. Although the NVC enhanced from 40 ppm to 4000 ppm, furthermore, the flow behaviour of the nanofluid inside the DASC remained almost the same. This is because the increase in the NVC causes most of the irradiation to be absorbed by the nanoparticles in the top layer.

Additionally, Fig. 8 exhibits the dissimilar nanoparticles' consequences on the volumetric absorbed irradiation. In the case of pure water (0 ppm) as the heat transfer fluid, a uniform volumetric heat generation is obtained because the radiation penetrates all over the collector (Fig. 7). The heat generation by the irradiance with the nanofluid shrinks to the collector's base, however, the utmost radiant heat flux and highest heat generation are obtained near the top partition.

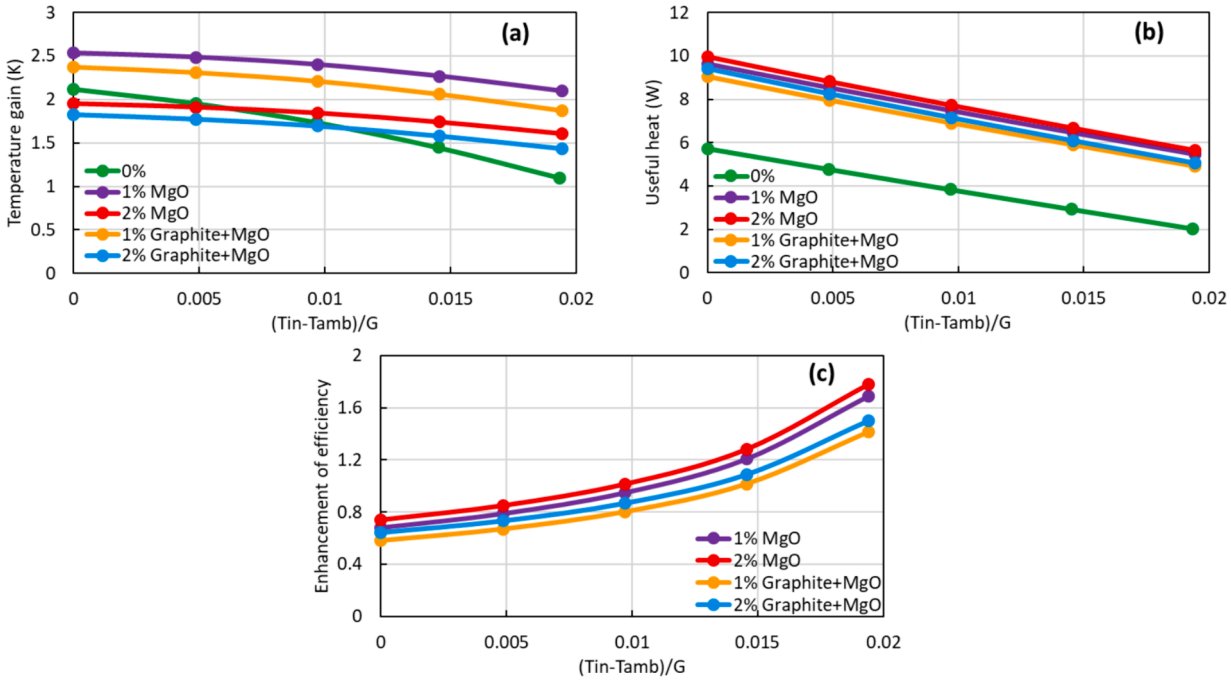

Fig. 16. Impact of the operating temperature on the PTCP (a) temperature rise, (b) heat gain, (c) enhancement of efficiency with varying inlet temperature.

4.3. Impact of hybrid nanoparticle type and volume concentration

As expressed in Fig. 6, the average PTCP of MgO nanoparticles is higher than the other nanoparticles, so it can be added to other nanofluids to enhance their performance. The PTCPs of hybrid/blended nanofluids are better than mono nanofluids (Fig. 9). The efficiency enhancement is 0.5, 0.4 and 0.6, respectively for water based TiO_2, Ag and Graphite nanofluids at NVC of 4 % whilst water based MgO/TiO_2, MgO/Ag, and MgO/Graphite fluids' efficiency enhancements are 0.6, 0.6, and 0.7, respectively. It is therefore a proof that hybrid nanofluids have stronger thermal performance at the same NVC due to the higher solar energy capture by improving the interaction of hybrid particles with irradiation. The PTCP of nanofluids is based on the optical and thermo-physical characteristics of the base liquid and nanoparticle types. Increasing the NVC enhances the PTCP of the collector by enhancing the nanofluid's radiation absorption power. The use of hybrid nanofluids at a constant NVC, therefore, further increases the capacity of this improvement. The hybrid nanofluids' absorption magnitude is equal to the mono nanoparticles that make up the blended nanoparticles. Thus, hybrid nanofluids absorb more solar irradiation, improving the PTCE. These hybrid particles' advantages on the thermal capacity confirms the findings of Kazaz *et al.* [28] who investigated that hybrid nanofluids augments the PTCP.

The temperature increment, on the other hand, is inversely proportional to the NVC as the nanofluid's flow rate augments, as the fluid moves rapidly inside the DASC, and the temperature rise diminishes as in Fig. 9(a). Thanks to the increased flow rate, however, the nanofluid's useful heat rate augments slowly with the NVC (Fig. 9(b)), increasing the photothermal conversion (Fig. 9(c)) and stored energy performances of the collector.

Fig. 10 displays the impact of different NVCs on the hybrid nanofluid. By adding nanoparticles and increasing their volume concentration, it is demonstrated that nanofluid absorbs more solar irradiation as it causes the maximum temperature to occur on the collector's top plate. As the NVC enhances, the heat generation by the radiation diminishes along the height of the collector, intensifying the radiation absorption in the upper wall (Fig. 11). Hence, the highest radiation flux and the maximum volumetric absorbed occur around the upper plate of the collector. Another important finding is that, as indicated in Fig. 10, a situation similar to Fig. 7 is obtained. That is, adding nanoparticles to water improves the absorption of sunbeam, while augmenting the NVC that prevents radiation from penetrating into the bottom layer of the collector.

As a final point in this regard is that the NVC increases the PTCE as seen in both the mono and hybrid nanofluids. This is understood by the fact that with the augmentation in the NVC, collision, and motion of particles in the nanofluid accelerate due to the Brownian motion and consequently, the surface volume ratio also increases. These improvements in the nanoparticles boost the nanofluid's thermal conductivity and thus enhance the PTCP by augmenting the heat transfer.

4.4. Impact of flow Reynolds number

The overall enhancement of the MgO/water and Graphite + MgO/water nanofluids is found to be better than the other types of nanofluids, therefore they are chosen for the further investigations as presented in this and following sub-sections.

The fluid's thermal performance is affected by the Reynolds number (Fig. 12). Because the fluid moves faster in the collector at high-speed values, the period of solar radiation that the fluid can absorb in the collector decreases. Accordingly, the working fluid's temperature gain diminishes (Fig. 12(a)), and the temperature propagation becomes more uniform inside the collector (Fig. 13). Moreover, as the fluid is more exposed to irradiation due to the lessening in the time spent inside the collector at low-speed values, the augmentation in the temperature gain results in the collector's upper surface temperature to increase (Fig. 13). Because this increase in temperature raises the thermal loss to the ambient, the heat absorption by the fluid inside the collector becomes less (Fig. 12b). Furthermore, increasing the mass flow rate results in lower temperature gradients. Thus, it improves the PTCP of the DASC by providing less thermal loss. This enhancement is confirmed by Vakili *et al.* [20] who discovered that the thermal capacity is improved with augmenting flow rate. As further demonstrated in Fig. 12(c), the augmentation increases slowly and the efficiency decreases for some cases in Fig. 12(c) is because it reveals the improvement of the nanofluid to water. For instance, when the Reynolds number develops from 0.2 to

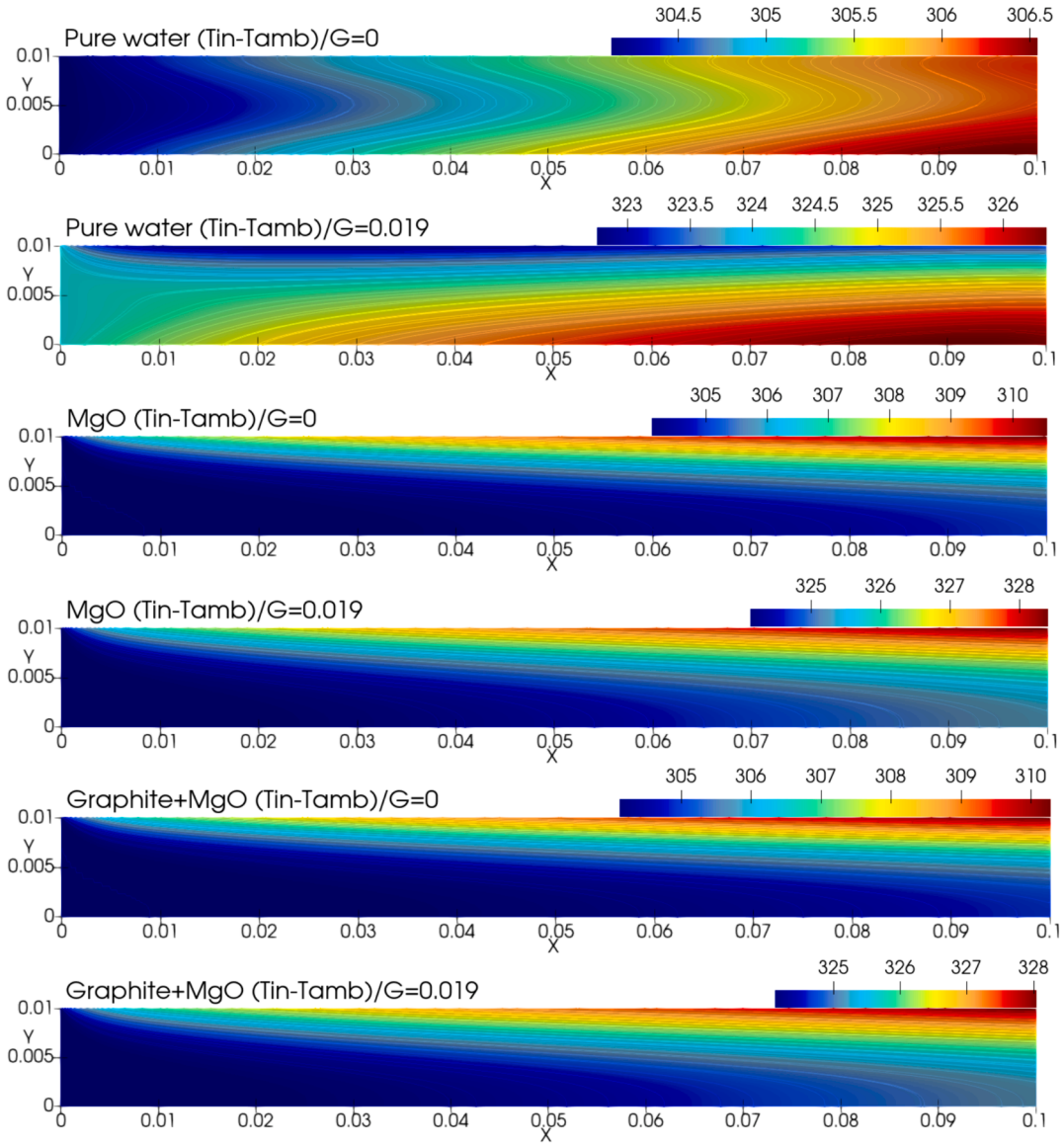

Fig. 17. Temperature (Kelvin, K) profiles of heat transfer fluid with varying inlet temperatures at NVC of 1%.

2, the efficiency of pure water improves from 0.11 to 0.44, while the efficiency of water based MgO nanofluid improves from 0.16 to 0.68, and the efficiency improvement appears to have decreased from 0.59 to 0.54. Similarly, the efficiency of water-based Graphite/MgO blended nanofluid rises from 0.15 to 0.62, and the efficiency improvement drops from 0.47 to 0.42. The possible reason for this diminishes in efficiency improvement may be the decrease in the rate of nanofluid thermal output to water.

Moreover, Fig. 14 clearly shows that even at a very small NVC, the addition of hybrid nanoparticles enhances the irradiance absorption capacity by approximately 2.5 times compared to water as the collision between the nanoparticles and light augments the light scattering. The light power, which decreases with the depth of the collector, however, causes the nanoparticles near the top plate to absorb more irradiation and generate more heat. Thus, more radiative heat flux can be obtained around the upper plate of the DASC as clarified in Fig. 14.

4.5. *Impact of particle size*

The nanoparticle size is another important point that could potentially influence the PTCE. The nanofluid's absorption coefficient is based on the particle size's square, whereas the scattering coefficient depends on its third power [39,28]. Thus, increasing particle size results in the improvement of the nanofluid's extinction coefficient enabling the nanofluid to absorb more solar irradiation. This provides to improve the absorption of nanoparticles and raises the temperature of the working fluid. Fig. 15 indicates that the PTCP slightly enhances with improving particle size for water based MgO and Graphite/MgO nanofluids. Since nanofluids with low volume concentration are exposed to solar radiation for a longer time throughout the collector, the temperature gain is higher when compared to the NVC of 3 % (Fig. 15(a)). Because the augmentation in NVC boosts the flow rate by accelerating the fluid, on the other hand, the rate of usable thermal energy is higher at high NVC (Fig. 15(b)). This ensures that the PTCP performance is higher at high NVCs, hence contributing to a greater enhancement of the thermal efficiency as demonstrated in Fig. 15(c) with enhancing the solar thermal capture of the collector. This development agrees with the findings of Tyagi *et al.* [5].

Furthermore, although the thermal coefficient of Graphite nanoparticles is about 43 times that of MgO nanoparticles, the PTCP of MgO/water nanofluid is greater than that of the MgO+Graphite/water nanofluid, as seen in Fig. 15. This may be because the hybrid nanofluids'

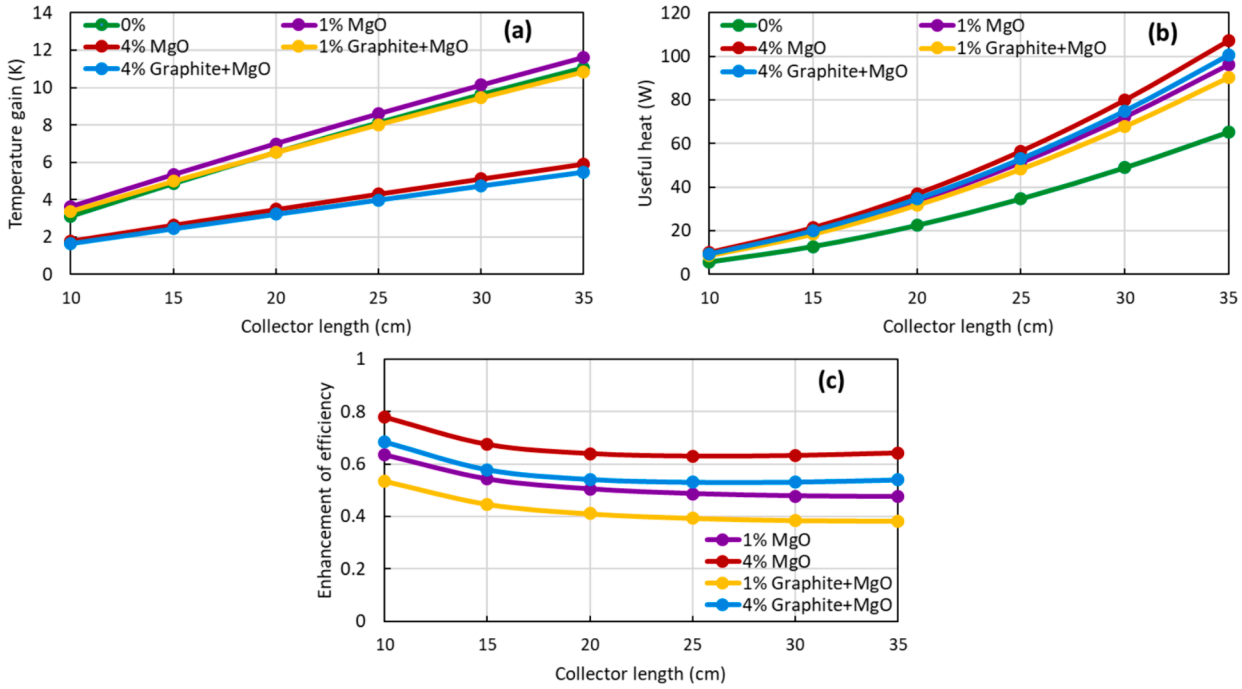

Fig. 18. Impact of the collector length on the PTCP (a) temperature rise, (b) heat gain, (c) enhancement of efficiency with varying collector length.

thermo-physical properties differ compared to single nanofluids. In addition, although the MgO+Graphite/water hybrid nanofluid's density and thermal conductivity increase, it is less than the water based MgO single nanofluid.

4.6. Impact of inlet temperature

The alteration of the base fluid's inlet/operating temperature is another point impacting the system performance as it alters the working fluid's thermo-physical characteristics. As the operating temperature enhances, the rise in the collector top plate temperature increases the thermal losses to the ambient, causing a decline in the fluid's temperature (Fig. 16(a) and Fig. 17). With this decrease, the heat absorption by the fluid in the collector by solar irradiation reduces (Fig. 16(b)). The decline in this absorbed heat causes a reduction in the PTCE. For instance, the efficiency of water for inlet temperatures of 304 K and 324 K is 0.55 and 0.19, respectively whereas the efficiency of 1 % MgO+-Graphite/water nanofluid is 0.87 and 0.47 %, respectively. This diminish endorses testimony from former observation of Gupta *et al.* [18]. In Fig. 16(c), however, it is noticed that the use of nanofluid increases with improving operating temperature, improving the efficiency of collector. This is because, as stated in Equation (23), when MgO/Graphite hybrid nanoparticles are added, it is seen that the efficiency improvements are 0.58 and 1.47 for the operating temperatures of 304 K and 324 K, respectively.

4.7. Impact of collector length

Fig. 18 displays the significance of the collector length on the PTCP. As the collector length augments, the capacity of solar irradiation collected by the collector boosts, so the fluid's temperature rise augments (Fig. 18(a)). Since the amount of heat gain that the fluid can utilize from solar energy also depends on this temperature rise, the working fluid's heat gain rate also raises with the increase in the collector length (Fig. 18(b)). While the collector length enhances, the thermal loss (combined radiation and convection) to the ambient augments since the DASC's top plate temperature increases, and the uniform temperature propagation inside the collector is also reduced. Due to high thermal loss, the PTCE diminishes, and the efficiency enhancement (Fig. 18(c)) of the collector diminishes with increasing length. This negative state in capacity accords with the investigation of Tyagi *et al.* [5].

5. Conclusions

A DASC using mono and blended nanofluids was investigated in this work. The impacts of NVC, which can be divided into two parts (low concentration and high concentration), type of nanoparticles (mono and hybrid nanoparticles), Reynolds number, nanoparticle size, operating temperature and collector size were examined. The radiative heat transfer model which includes the effects of absorption, scattering and emitting and fluid flow and governing equations were resolved using Ansys Fluent. Numerical results presented that the nanoparticle addition developed the fluid's absorption capability of solar radiation due to the radiation-nanoparticle interaction, thus enhancing the PTCE. This enhancement was further improved by using hybrid nanoparticles since their extinction coefficient is higher than the mono nanoparticles. It was determined that the most important element influencing the PTCP was thermal loss to the environment. It was revealed that as the NVC augmented from 1 % to 4 %, the top plate temperature of the DASC lessened, thereby reducing the thermal loss capacity. Besides, the decrease or rise in the fluid velocity inside the collector altered the time that the working fluid was exposed to irradiation density. As the Reynolds number develops from 0.2 to 2, the efficiency of pure water and MgO/water nanofluid is enhanced by 300 % and 325 % respectively.

Moreover, developing the NVC caused the nanoparticles near the top wall to absorb more sunbeam. This diminished the heat generation by the sunbeam as it moved towards the bottom of the collector. The increment in the PTCE was observed as the enhancement in the nanoparticle diameter helps the nanofluid to improve its optical properties. This enhances the nanoparticles' absorption and further increases the working fluid's temperature. While the rate of heat absorbed by the fluid declined with the development in the operating temperature, this rate increased with the boost of the collector length. Since an enhanced operating temperature increases the heat loss from the collector to the environment, the fluid's temperature diminishes. When the fluid's inlet

temperature augments from 304 K to 324 K, the overall system efficiency decreases by 2.9 times and 1.9 times for pure water and MgO+Graphite/water hybrid nanofluid, respectively. Further, due to the high thermal loss, the PTCE diminishes, as a results the efficiency enhancement of the collector diminishes with increasing length. As the NVC also enhanced, the heat transfer enhancement is improved as a result of the thermal conductivity augmentation due to the Brownian movement of nanoparticles.

CRediT authorship contribution statement

Oguzhan Kazaz: Writing – review & editing, Writing – original draft, Visualization, Validation, Software, Methodology, Investigation, Formal analysis, Conceptualization. **Nader Karimi:** Writing – review & editing, Supervision. **Manosh C. Paul:** Writing – review & editing, Supervision, Resources, Project administration, Funding acquisition, Conceptualization.

Declaration of competing interest

The authors declare that they have no known competing financial interests or personal relationships that could have appeared to influence the work reported in this paper.

Data availability

Data will be made available on request.

References

[1] O. Kazaz, N. Karimi, M.C. Paul, Optically functional bio-based phase change material nanocapsules for highly efficient conversion of sunlight to heat and thermal storage, Energy 305 (2024) 132290.

[2] O. Kazaz, N. Karimi, S. Kumar, G. Falcone, M.C. Paul, Thermally enhanced nanocomposite phase change material slurry for solar-thermal energy storage, J. Storage Mater. 78 (2024) 110110.

[3] Q. He, S. Wang, S. Zeng, Z. Zheng, Experimental investigation on photothermal properties of nanofluids for direct absorption solar thermal energy systems, Energ. Conver. Manage. 73 (2013) 150–157.

[4] O. Kazaz, N. Karimi, S. Kumar, G. Falcone, M.C. Paul, Effects of nanofluid's base fluid on a volumetric solar collector, IET Conference Proceedings 2022 (11) (2022) 1–3.

[5] H. Tyagi, P. Phelan, R. Prasher, Predicted efficiency of a Low-temperature nanofluid-based direct absorption solar collector, J. Sol. Energy Eng. 131 (4) (2009) 041004.

[6] R.A. Taylor, P.E. Phelan, T.P. Otanicar, C.A. Walker, M. Nguyen, S. Trimble, R. Prasher, Applicability of nanofluids in high flux solar collectors, J. Renewable Sustainable Energy 3 (2011) 023104.

[7] O. Kazaz, R. Ferraro, M. Tassieri, S. Kumar, G. Falcone, N. Karimi, M.C. Paul, Sensible heat thermal energy storage performance of mono and blended nanofluids in a free convective-radiation inclined system, Case Studies in Thermal Engineering 51 (2023) 103562.

[8] O. Kazaz, N. Karimi, S. Kumar, G. Falcone, M.C. Paul, Heat transfer characteristics of fluids containing paraffin core-metallic shell nanoencapsulated phase change materials for advanced thermal energy conversion and storage applications, J. Mol. Liq. 385 (2023) 122385.

[9] T.P. Otanicar, P.E. Phelan, J.S. Golden, Optical properties of liquids for direct absorption solar thermal energy systems, Sol. Energy 83 (7) (2009) 969–977.

[10] O. Kazaz, N. Karimi, G. Falcone, S. Kumar and M. C. Paul, "Effect of Radiative Heat Transfer in Nanofluid for Volumetric Solar Collector," *Energy Proceedings,* vol. 21, 2021.

[11] P. Cao, Y. Li, Y. Wu, H. Chen, J. Zhang, L. Cheng, T. Niu, Role of base fluid on enhancement absorption properties of Fe3O4/ionic liquid nanofluids for direct absorption solar collector, Sol. Energy 194 (2019) 923–931.

[12] M. Karami, M. Raisee, S. Delfani, M.A. Akhavan Bahabadi, A.M. Rashidi, Sunlight absorbing potential of carbon nanoball water and ethylene glycol-based nanofluids, Opt. Spectrosc. 115 (2013) 400–405.

[13] Y. Gan, L. Qiao, Optical properties and radiation-enhanced evaporation of nanofluid fuels containing carbon-based nanostructures, Energy Fuel 26 (7) (2012) 4224–4230.

[14] C. Qin, J.B. Kim, H. Gonome, B.J. Lee, Absorption characteristics of nanoparticles with sharp edges for a direct-absorption solar collector, Renew. Energy 145 (2020) 21–28.

[15] A. Gimeno-Furió, R. Martínez-Cuenca, R. Mondragón, A.F.V. Gasulla, C. Doñate-Buendía, G. Mínguez-Vega, L. Hernández, Optical characterisation and photothermal conversion efficiency of a water-based carbon nanofluid for direct solar absorption applications, Energy 212 (2020) 118763.

[16] H. Wang, X. Li, B. Luo, K. Wei, G. Zeng, The MXene/water nanofluids with high stability and photo-thermal conversion for direct absorption solar collectors: a comparative study, Energy 227 (2021) 120483.

[17] G. Zhu, L. Wang, N. Bing, H. Xie, W. Yu, Enhancement of photothermal conversion performance using nanofluids based on bimetallic Ag-Au alloys in nitrogen-doped graphitic polyhedrons, Energy 183 (2019) 747–755.

[18] H.K. Gupta, G.D. Agrawal, J. Mathur, Experimental study of water-Based Al2O3 nanofluid flow in direct absorption solar collector, Macromol. Symp. 357 (2015) 30–37.

[19] P.P. Thakur, T.S. Khapane, S.S. Sonawane, Comparative performance evaluation of fly ash-based hybrid nanofluids in microchannel-based direct absorption solar collector, J. Therm. Anal. Calorim. 143 (2021) 1713–1726.

[20] M. Vakili, S.M. Hosseinalipour, S. Delfani, S. Khosrojerdi, M. Karami, Experimental investigation of graphene nanoplatelets nanofluid-based volumetric solar collector for domestic hot water systems, Sol. Energy 131 (2016) 119–130.

[21] P. Raj, S. Subudhi, A review of studies using nanofluids in flat-plate and direct absorption solar collectors, Renew. Sustain. Energy Rev. 84 (2018) 54–74.

[22] Ansys, Fluent User's Guide, ANSYS Inc, Canonsburg, 2013.

[23] C.F. Bohren, D.R. Huffman, Absorption and scattering of Light by small particles, Wiley, New York, 1983.

[24] G.M. Hale, M.R. Querry, Optical constants of water in the 200-nm to 200-μm wavelength region, Appl. Opt. 12 (3) (1973) 555–563.

[25] S. Babar, J.H. Weaver, Optical constants of Cu, Ag, and Au revisited, Appl. Opt. 54 (3) (2015) 477–481.

[26] E.D. Palik, Handbook of Optical Constants of Solids, Academic Press, 1997.

[27] J.A. Duffie, W.A. Beckman, Solar engineering of thermal processes, John Wiley & Sons Inc, Hoboken, New Jersey, 2013.

[28] O. Kazaz, N. Karimi, S. Kumar, G. Falcone, M.C. Paul, Enhanced sensible heat storage capacity of nanofluids by improving the photothermal conversion performance with direct radiative absorption of solar energy, J. Mol. Liq. 372 (2023) 121182.

[29] O. Kazaz, N. Karimi, S. Kumar, G. Falcone, M.C. Paul, Effects of combined radiation and forced convection on a directly capturing solar energy system, Thermal Science and Engineering Progress 40 (2023) 101797.

[30] Y.A. Cengel, B.S. Klein, Heat transfer: a practical approach, WBC McGraw-Hill, Boston, 1998.

[31] B. Ghasemi, S.M. Aminossadati, Periodic natural convection in a nanofluid-filled enclosure with oscillating heat flux, Int. J. Therm. Sci. 49 (1) (2010) 1–9.

[32] R. Davarnejad, M. Jamshidzadeh, CFD modeling of heat transfer performance of MgO-water nanofluid under turbulent flow, Engineering Science and Technology, an International Journal 18 (4) (2015) 536–542.

[33] M. Sheikholeslami, D.D. Ganji, H.R. Ashorynejad, Investigation of squeezing unsteady nanofluid flow using ADM, Powder Technol. 239 (2013) 259–265.

[34] H. Duan, R. Chen, Y. Zheng, C. Xu, Photothermal properties of plasmonic nanoshell-blended nanofluid for direct solar thermal absorption, Opt. Express 26 (3) (2018) 29956–29967.

[35] T.P. Otanicar, P.E. Phelan, R.S. Prasher, G. Rosengarten, R.A. Taylor, Nanofluid-based direct absorption solar collector, J. Renewable Sustainable Energy 2 (3) (2010) 033102–033113.

[36] M. Du, G.H. Tang, Plasmonic nanofluids based on gold nanorods/nanoellipsoids/nanosheets for solar energy harvesting, Sol. Energy 137 (2016) 393–400.

[37] C.V. Vital, S. Farooq, R.E. de Araujo, D. Rativa, L.A. Gómez-Malagón, Numerical assessment of transition metal nitrides nanofluids for improved performance of direct absorption solar collectors, Appl. Therm. Eng. 190 (2021) 116799.

[38] H.M.F. Rabbi, A.Z. Sahin, B.S. Yilbas, A. Al-Sharafi, Methods for the determination of nanofluid optical properties: a review, Int. J. Thermophys. 42 (9) (2021) 1–42.

[39] O. Kazaz, N. Karimi, S. Kumar, G. Falcone, M.C. Paul, "Numerical ınvestigation of the ınfluences of nanoparticle size and tilt angle in a directly absorption solar system", in *14th International Conference on Applied Energy (ICAE2022)*, Bochum, Germany, 2022.